Hindawi
Geofluids
Volume 2023, Article ID 1652890, 7 pages
https://doi.org/10.1155/2023/1652890

Research Article

Rapid and Slow Unlocking-Induced Startup Mechanisms of Locked Segment-Dominated Landslides

Hongran Chen,[1,2] **Chao Xu**,[1,2,3] **Yuan Cui**,[1,2,3] **and Siqing Qin**[1,2,3]

[1]*Key Laboratory of Shale Gas and Geoengineering, Institute of Geology and Geophysics, Chinese Academy of Sciences, Beijing 100029, China*
[2]*Innovation Academy for Earth Science, CAS, Beijing 100029, China*
[3]*College of Earth and Planetary Sciences, University of Chinese Academy of Sciences, Beijing 100049, China*

Correspondence should be addressed to Siqing Qin; qsqhope@mail.iggcas.ac.cn

Received 9 September 2022; Accepted 10 October 2022; Published 24 March 2023

Academic Editor: Yiding Bao

Locked segment-dominated landslides initiate when locked segments are sufficiently damaged to be unlocked. The evolution of such slopes toward instability displays either an exponentially or stepwise accelerated displacement pattern, but the underlying mechanisms of these patterns are elusive. We show that the displacement pattern is governed by mechanical synergy (resistance homogenization) between the ruptured locked segment and the transfixion segment. Using a mechanical model, we demonstrate that rapid and slow resistance homogenizations, which depend mainly on the brittleness of locked segments, cause two unlocking-induced startup mechanisms that lead to loss of slope stability: one occurring at the peak-stress points and the other at the residual-strength points of the locked segments. Accordingly, the evolution toward instability exhibits one of the two abovementioned patterns. External factors, such as rainwater, can deteriorate the strength of geomaterials but hardly alter the inherent mechanical rules that a locked segment adheres to. These findings provide insights into the mechanism of locked segment-dominated landslides and pave the way for reliably predicting their occurrence.

1. Introduction

Many slopes worldwide are stabilized by locked segments, i.e., geological structures with high bearing capacity (determined by scale and strength) along potential slip surfaces [1, 2]. Such a slope becomes unstable only when a locked segment becomes unlocked (fails). Rock bridges [3] are the most common locked segments in rock slopes [4–6]. An example is the Yanchihe slope in Hubei, China (E117.298°, N31.208°, Figure 1(a), [7]). Locked segments also exist in Quaternary sedimentary slopes such as the Longxi slope (E100.883°, N36.102°, Figure 1(b), [8]) in the Longyangxia Reservoir area on the Yellow River.

Gradual damage of locked segments can cause growing displacement of the corresponding slopes. Therefore, a roughly unified displacement pattern is expected, and the quite different displacement patterns of the Yanchihe and Longxi slopes as they evolved toward instability are difficult to explain. The Yanchihe slope displaced with an exponentially accelerated trend (Figure 2(a), [7]), whereas the acceleration displacement of the Longxi slope was suspended and then resumed, thus exhibiting a stepwise accelerated curve (Figure 2(b), [8]). As both patterns are widely observed in locked segment-dominated landslides, uncovering their corresponding mechanisms is crucial for reliable landslide prediction. If the formations of these patterns remain elusive, then whether displacement acceleration of a locked segment-dominated slope indicates a forthcoming landslide cannot be correctly prejudged.

The transfixion of slip surfaces is either progressive or instantaneous, depending on the physical properties of materials on the slip surfaces [9, 10]. Accelerated cracking of a locked segment can result in an exponentially accelerated displacement curve [11] but cannot explain a stepwise accelerated curve. A stepwise accelerated displacement pattern is usually assumed to be derived from the pore-water

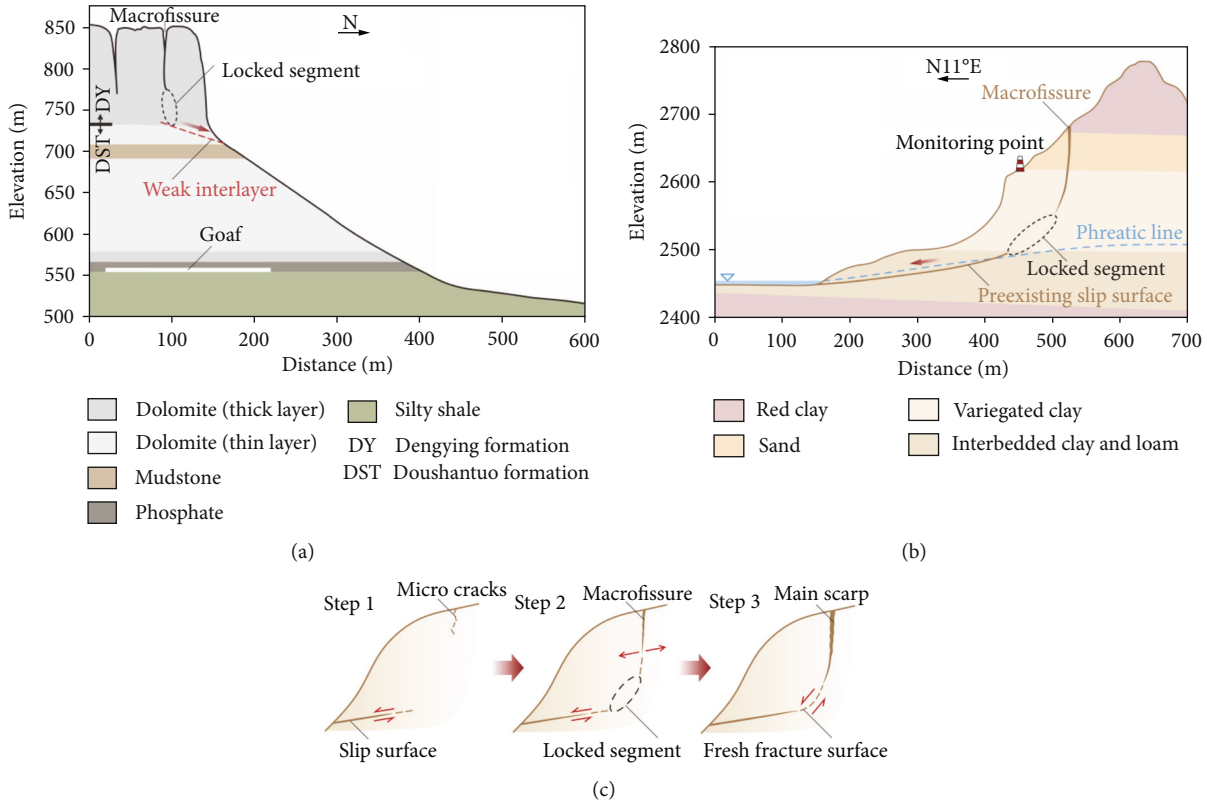

FIGURE 1: Geological profiles of the (a) Yanchihe [7] and (b) Longxi slopes [8], and (c) typical formation and failure processes of a locked segment. Step 1: a bottom slip surface develops or preexists. Step 2: tension cracks form a macrofissure with slope deformation, where the intact part between the fissure and bottom slip surface serves as a locked segment. Step 3: the locked segment becomes unlocked and landslide occurs.

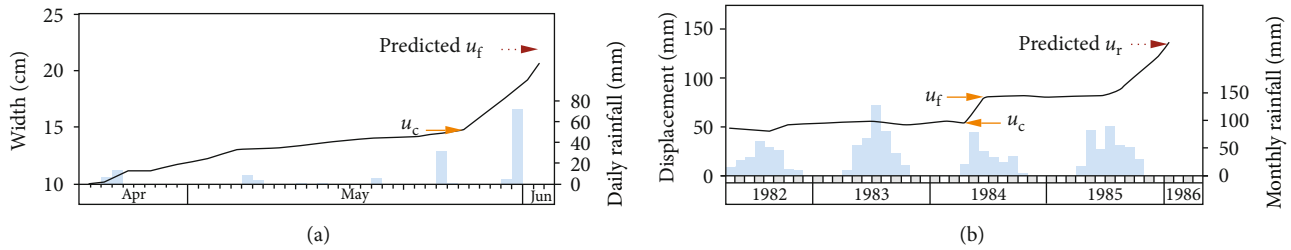

FIGURE 2: Displacement–time curves of the (a) Yanchihe [7] and (b) Longxi slopes [8]. The blue bars are the rainfall amounts.

pressure growth and strength degradation of geomaterials along a potential slip surface due to heavy rainfall [12]. However, the behavior of the Longxi slope contradicted this assumption because its displacement remained nearly unchanged under the heavy rainfall in July 1983, but substantial displacement was observed in May 1984 following less precipitation. Furthermore, the Longxi landslide occurred against the backdrop of the dry season in 1986. These paradoxes suggest that rainfall is not the key factor dominating the slope displacement patterns.

Physical modeling tests of antidip soft-hard interbedded rock slopes [13–15] show that soft-layer deformation is constrained by the hard layers until the hard layers break, suggesting that the interaction between different media on a potential slip surface is key to the displacement behavior of the slope. As the potential slip surface of a slope comprises a strong medium (locked segment) and a weak medium (transfixion segment), the mechanisms corresponding to the two patterns inherently involve mechanical synergy between the strong and weak media, which possess distinct mechanical properties [16, 17]. We will investigate this synergy on the aforementioned two slopes as typical examples.

2. Formation and Mechanical Behaviors of Locked and Transfixion Segments

The locked segments in the Yanchihe and Longxi slopes were formed by similar processes (Figure 1(c), [18]). In the Yanchihe phosphate mine, roof subsidence of the goaf caused slippage of the sliding mass along a weak interlayer of muddy dolomite affected by karstification (bottom slip

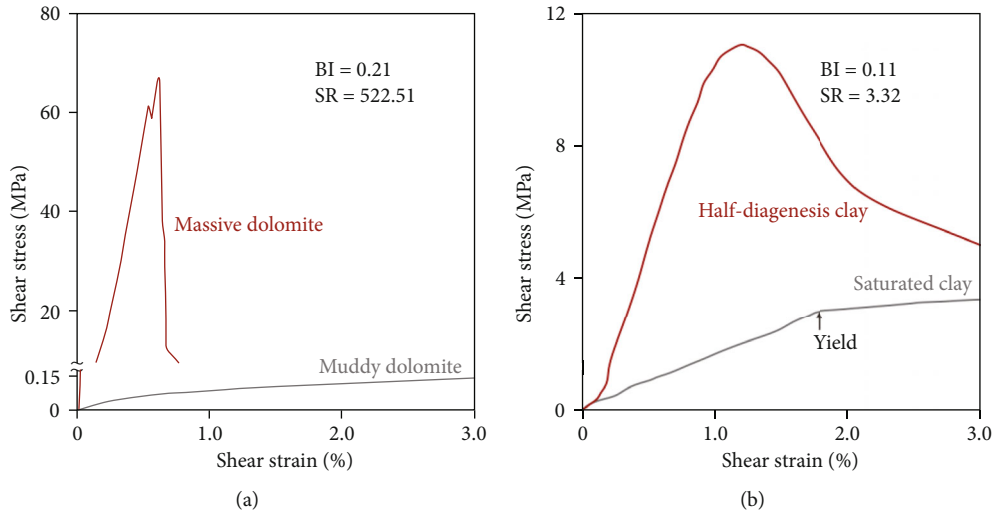

FIGURE 3: Shear stress–strain relations of the strain-softening strong media constituting locked segments (red curves) and strain-hardening weak media filling the lower transfixion segments (gray curves) on the slip surfaces of the (a) Yanchihe [21] and (b) Longxi slopes [8]. BI denotes the brittleness index [22] of the strong media (where a greater BI indicates a higher brittleness), and SR denotes the shear strength ratio of strong medium to weak medium.

surface) [19], generating tension cracks in the upper slope. As the slope deformed, the cracks connected to form a macrofissure. On its south side is the rough shovel-shaped main scarp of the landslide [1]. The relatively intact massive dolomite between the fissure and interlayer served as a locked segment. On the Longxi slope, a bottom slip is developed through strength degradation of the saturated water-sensitive clay along the phreatic line [19]. Upper tensile cracks were then produced by movement of the slope along the slip surface and gradually coalesced into a macrofissure. On its south side, the main scarp is similar to that of the Yanchihe slope. A locked segment thereby formed between the two transfixion segments.

The locked segments were gradually damaged under shear stress and external factors (e.g., rainfall). Eventually, the damage was sufficient to cause unlocking, which was quickly followed by catastrophic landslides. After the landslide events, shear striations were observed on both the middle and lower slip surfaces [20], but only the fracture surfaces at the speculated locations of the locked segments were fresh [8]. These facts confirm the existence of locked segments that underwent shear rupture and slip while the lower transfixion segments experienced shear dislocation.

Because the two lateral surfaces of an open tensile fissure (upper transfixion segment) hardly contact each other, this segment experiences negligible antisliding force. On the Yanchihe and Longxi slopes, the weak media on the lower transfixion segments are muddy dolomite and saturated clay, respectively, whereas the strong media constituting the locked segments are massive dolomite and compact half-diagenesis clay, respectively. In geotechnical tests [8, 21], the weak media with lower stiffness and strength exhibited strain-hardening properties whereas the strong media with higher strength and stiffness exhibited strain-softening properties (Figure 3).

3. Mechanical Synergy between Strong and Weak Media on Potential Slip Surface

The shear stress along a potential slip surface of slope naturally concentrates on a strong locked segment preceding its rupture at the peak-stress point. Thus, the mechanical synergy between strong and weak media is feeble in this stage, and the slope's displacement pattern is controlled by the locked segment. Under the combined effects of shear stress and external factors, the locked segment becomes damaged by crack growth. Unstable crack growth initiating from the volume-expansion point in the locked segment (point C in Figure 4) cannot be restrained even under a constant applied load [23]. Thus, the volume-expansion point corresponds to the onset of displacement acceleration of a locked segment-dominated slope. Once a damaged strain-softening locked segment reaches its peak-stress point (point D in Figure 4), it ruptures and the resulting stress drop causes partial transfer of the applied load to the weak medium on a lower transfixion segment, which subsequently yields. Such mechanical synergy between the strong and weak media homogenizes the distribution of shear resistance along a through-going slip surface; hence, it is referred to as resistance homogenization.

The massive dolomite is much stronger than the muddy dolomite on the lower transfixion segment on the Yanchihe slope. When ruptured at its peak-stress point, the massive dolomite generates a large, rapid post-peak stress drop and then it holds low residual strength, due to its high brittleness (Figure 3(a)). As a result of the large stress drop, most of its load is transferred to the weak medium, which then yields rapidly. In this context, the small resistance increase of the strain-hardening weak medium cannot offset the large resistance decrease of the locked segment during resistance homogenization, meaning that the total antisliding force decreases along the through-going slip

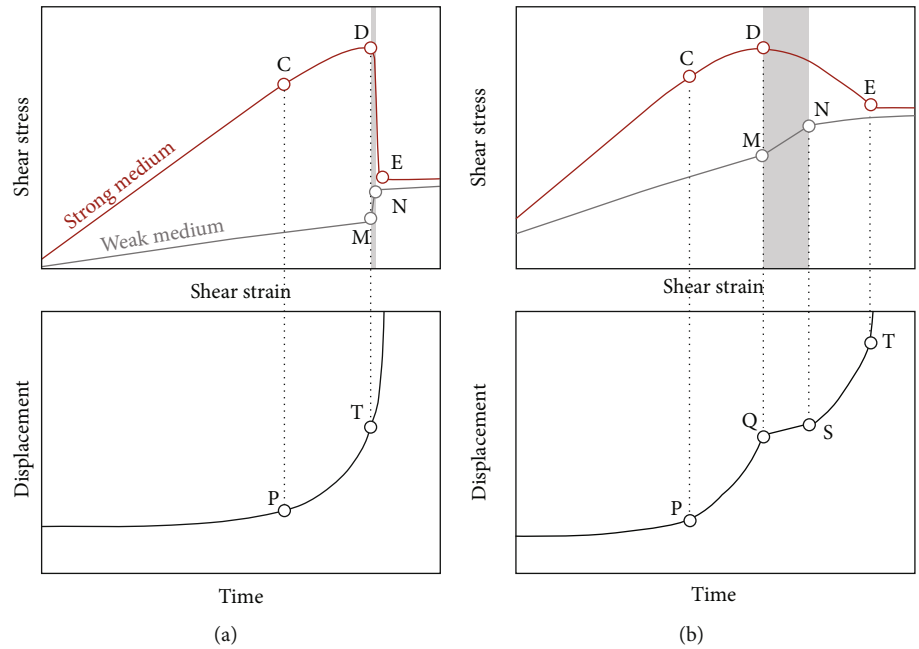

Figure 4: Shear stress–strain and displacement–time relations corresponding to (a) rapid and (b) slow unlocking-induced startup mechanisms. Points C, D, and E denote the volume-expansion, peak-stress, and residual-strength points of the locked segments, respectively. Points M and N denote the onset and termination, respectively, of the resistance homogenization process (gray shaded area). Points P and T denote the startups of displacement acceleration and landslide, respectively. In (b), points Q and S denote the suspension and resumption of displacement acceleration, respectively.

surface. Consequently, the displacement acceleration cannot be restrained, and the evolution of the Yanchihe slope tends toward instability. Between the peak-stress and residual-strength points of the locked segment, the displacement increase during the transient-unloading phase is minimal and slope instability develops; therefore, the peak-stress point can be viewed as the unlocking point of the locked segment. Such a mechanism following rapid homogenization is referred to as rapid unlocking-induced startup (Figure 4(a)).

Compared to the strong and weak media on the Yanchihe slope, the compacted half-diagenesis clay (locked segment) on the Longxi slope has lower brittleness and smaller strength and stiffness differences between the strong and weak media (Figure 3(b)). Therefore, when the locked segment ruptures, a small and gentle post-peak stress drop and a correspondingly slow and steady load transfer to the weak medium are expected. The weak medium should respond to this load transfer with a modest shear stress growth rate. In addition, given the much larger scale of the lower transfixion segment than the locked segment, the larger resistance increase of the weak medium can slightly overcompensate the smaller resistance decrease of the ruptured locked segment until the end of resistance homogenization, thereby achieving equilibrium between the resistance increase and decrease. Under this circumstance, the slow homogenization can suspend the displacement acceleration over an extended period. After homogenization, the displacement acceleration resumes because the resistance decrease of the locked segment is no longer offset by the resistance increase of the weak medium. When the total resistance reaches its minimum at the residual-strength point of the locked segment, slope instability will quickly follow. As such, if the displacement is stepwise accelerated, a locked segment might be unlocked at its residual-strength point. Such a mechanism following slow homogenization is here called slow unlocking-induced startup (Figure 4(b)).

4. Analysis and Results

The peak-stress and residual-strength points are two key characteristic points that indicate the instability of locked segment-dominated slopes following the rapid and slow unlocking-induced mechanisms, while displacement acceleration at the volume-expansion point preceding the two points can serve as their discernible precursor. If the mechanical relationships among these points are established, the displacement values at the first two points can be obtained based on those at the volume-expansion point. This will help in quantitatively determining the unlocking-induced mechanism of a locked segment-dominated slope.

By coupling a damage-constitutive model based on the Weibull distribution with the one-dimension renormalization group model, we obtained the theoretical expressions of displacements u_c, u_f, and u_r corresponding to the volume-expansion, peak-stress, and residual-strength points of the locked segment along the slip surface, respectively [2], and the displacement ratios of u_f/u_c and u_r/u_c exclusively depend on the parameter m and are formulated as [2, 24, 25]

$$\frac{u_f}{u_c} = \left(\frac{2^m - 1}{m \ln 2}\right)^{1/m}, \quad (1)$$

$$\frac{u_r}{u_c} = \left[\frac{(m+1)(2^m - 1)}{m \ln 2}\right]^{1/m}. \quad (2)$$

The parameter m characterizes the shapes of the stress–strain curves of geomaterials under various conditions (e.g., heterogeneity, loading rate, and moisture content), and a high m value corresponds to a sharp shape suggesting high brittleness. Therefore, it can comprehensively reflect the effect of various internal and external factors on the damage behavior of a locked segment. Because a locked segment contains massive joints and fissures serving as rainwater flow channels [26], it is with a certain water content. Furthermore, the locked segment is subjected to an extremely slow shear loading rate. Under these circumstances, the shape of its stress–strain curve can be gentle with a slow and small post-peak stress drop (Figure 5) [27, 28], which corresponds to a low m value. The specific reasonable range of m value, as Yang et al. [29] demonstrated, is 1.0–4.0. Because the two displacement ratios are insensitive to variations in the m value, they can be approximately expressed in terms of their average values within the range [25, 30]. Thus, Eqs. (1) and (2) are simplified as [2, 24, 25]

$$u_f = 1.48u_c, \quad (3)$$

$$u_r = 2.49u_c. \quad (4)$$

The reliability of this model has been validated in retrospective analyses of several locked segment-dominated landslides [24, 25]. Drawing on this model and on monitored displacement data, we can reveal the evolutionary mechanisms of the Yanchihe and Longxi landslides and test the hypothesis that the exponentially and stepwise accelerated displacement curves correspond, respectively, to rapid and slow unlocking-induced startup mechanisms.

The displacement of the Yanchihe locked segment along the slip surface is represented by the macrofissure width (Figure 1(a)). The width began exponentially increasing from May 24 of 1980, causing minor rockfalls [19]. This finding suggests that the volume-expansion point of the locked segment was attained at this time. The width at the peak-stress point of the locked segment determined by Eq. (3) approximately equals the value measured on June 2 of 1980 (Figure 2(a)), when rock-cracking noises were heard throughout the night [19]. Therefore, the locked segment was unlocked on that day and was succeeded by a 1 Mm^3 landslide at dawn on the following day. These results confirm that the peak-stress point of the locked segment corresponded to the startup of the Yanchihe landslide, and that an exponential evolution of the slope toward instability followed the rapid unlocking-induced startup mechanism.

The displacement of the Longxi slope, recorded at a monitoring point above the locked segment, began accelerating on April 1 of 1984 (Figure 2(b)) and was suspended from June 2 of 1984, as evidenced by the deflection of the displacement curve at that time. The sliding mass then rotated and began moving along the slip surface, accompanied by ground upheaval at the slope foot [20]. These phenomena suggest that the locked segment was damaged to reach its peak-stress point, from which the applied load was partially transferred to the weak medium on the lower transfixion segment, thereby causing slow resistance homogenization and displacement acceleration suspension. The displacement acceleration following the homogenization termination resumed from July 1 of 1985 and was followed by a 1.5 Mm^3 landslide. Therefore, the displacement before the landslide manifested a stepwise accelerated profile. The displacement value at the residual-strength point calculated by Eq. (4) approximates the measured value one week prior to the landslide (Figure 2(b)), confirming that the Longxi slope instability followed the slow unlocking-induced startup mechanism.

5. Discussion

Large-scale locked segment-dominated slopes have been widely reported worldwide. For example, ruptured locked segments caused major rockslides in the Canadian Rocky Mountains [31], Alps Mountains [5], and Tibet Plateau [1]. Because locked segments with high bearing capacity can accumulate abundant elastic strain energy, their unlocking often induces devastating high-speed and long-runout landslides [18, 32]. Therefore, uncovering the unlocking-induced startup mechanisms of such slopes has global implications for mitigating landslide hazards.

As explained above, the brittleness of locked segments crucially influences the magnitude and duration of the post-peak stress drop. Higher brittleness usually corresponds to higher strength and a larger stress drop. Thus, the unlocking-induced startup mechanism and displacement pattern of a slope are governed mainly by the brittleness of the locked segment. This understanding is mainly supported by site observations and mechanical analyses. To further consolidate the relationships between displacement patterns and unlocking-induced startup mechanisms and to discover essential factors governing these mechanisms, more evidence needs to be acquired via other methods, such as physical modeling experiments and numerical simulations.

Displacement of a locked segment-dominated slope usually follows damage accumulation in the locked segment. Damages are sourced from the self-weight of the slope mass and from external factors, especially rainfall. Water can strongly deteriorate the strength of geomaterials through the fatigue effect [33] and chemical alteration [34]. Moreover, water can raise the pore pressure on slip surfaces [35], thereby reducing their intergranular frictional resistance and structural stability. For instance, karstification can spread etch pits on dolomite cleavage and cause its disintegration [36]; the dissolution of the inorganic salt can decline the cohesion of the saturated clay on the Longxi slope by 27–50% [8]. Under these effects, the damage of a locked segment can reach certain mechanical characteristic points, each corresponding to a specific mechanical behavior. For instance, displacement begins accelerating at the

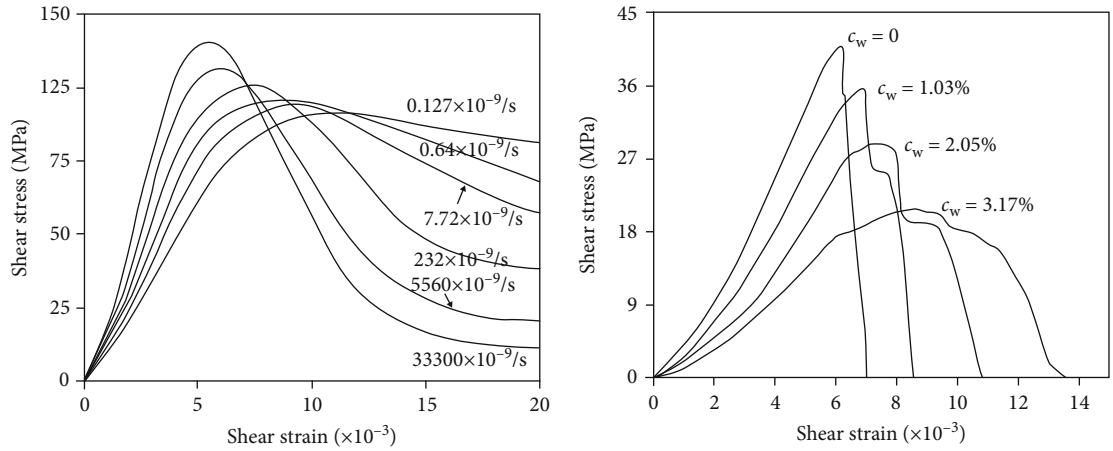

Figure 5: Shear stress–strain curves of rocks for various (a) strain rates [27] and (b) water contents (c_w) [28]. Slower loading rates and higher water contents result in less sharp curves, which correspond to lower m values.

volume-expansion point, and catastrophic slip begins at the peak-stress point or residual-strength point. Once these points are reached, the corresponding behaviors are inevitable even without the effects of external factors, because the locked segment can spontaneously crack from its volume-expansion point under the self-weight of a slope. Thus, the displacement of the Longxi slope began speeding up when the volume-expansion point of the locked segment was reached in May of 1984, although the precipitation was below the maximum precipitation in 1983; the Longxi slope evolved uncontrollably toward instability, and its catastrophic slip occurred during a three-month-long rainless period (total precipitation < 4 mm from November 1985 to January 1986) rather than during a wet season. Indeed, the damage behavior of the locked segment governs the evolution of a locked segment-dominated slope toward instability, as described by the constant displacement ratios. Therefore, locked segment-dominated landslides are predictable based on firm physical principles.

To reliably assess the stability of a locked segment-dominated slope, one must investigate the distributions of the locked and transfixion segments and the mechanical properties of media on a potential slip surface. The unlocking-induced startup mechanism of a slope can be prejudged on this basis. Moreover, we highlight that damage should be reliably detected by setting monitoring points on the locked segment.

6. Conclusions

Large-scale locked segment-dominated slopes are extensively distributed worldwide. Governed by their brittleness, locked segments are unlocked at either their peak-stress or residual-strength points, causing impending landslides. Accordingly, the startup mechanism of the landslides can be rapid with an exponentially accelerated displacement pattern or slow with a stepwise accelerated displacement pattern. However, as mentioned above, further insights into the relationships between the unlocking process, displacement pattern, and startup behavior are still required.

The results of this study demonstrate that locked segment-dominated landslides obey certain mechanical rules and can, thus, be reliably predicted.

Data Availability

The precipitation data were downloadable for registered members of the China Meteorological Data Service Centre (http://data.cma.cn/en). The displacement and mechanical experimental data were derived from published literatures.

Conflicts of Interest

The authors declare that they have no conflicts of interests.

Authors' Contributions

S. Qin initiated the study. S. Qin and H. Chen developed the structure of the study. H. Chen, C. Xu, and Y. Cui analyzed the data and interpreted the results. H. Chen wrote the original manuscript. All authors discussed the results and revised the manuscript.

Acknowledgments

This work was supported by the National Natural Science Foundation of China (nos. 42090052 and 42107184).

References

[1] R. Huang, "Mechanisms of large-scale landslides in China," *Bulletin of Engineering Geology and the Environment*, vol. 71, no. 1, pp. 161–170, 2012.

[2] S. Qin, Y. Wang, and P. Ma, "Exponential laws of critical displacement evolution for landslides and avalanches," *Chinese Journal of Rock Mechanics and Engineering*, vol. 29, no. 5, pp. 873–880, 2010.

[3] K. Terzaghi, "Stability of steep slopes on hard unweathered rock," *Géotechnique*, vol. 12, no. 4, pp. 251–270, 1962.

[4] D. Elmo, D. Stead, B. Yang, G. Marcato, and L. Borgatti, "A new approach to characterise the impact of rock bridges in stability analysis," *Rock Mechanics and Rock Engineering*, vol. 55, pp. 2551–2569, 2021.

[5] M. Frayssines and D. Hantz, "Failure mechanisms and triggering factors in calcareous cliffs of the subalpine ranges (French Alps)," *Engineering Geology*, vol. 86, no. 4, pp. 256–270, 2006.

[6] C. Lévy, L. Baillet, D. Jongmans, P. Mourot, and D. Hantz, "Dynamic response of the Chamousset rock column (Western Alps, France)," *Journal of Geophysical Research: Earth Surface*, vol. 115, no. F4, 2010.

[7] Y. Sun and B. Yao, "Study on mechanism of the rockslide at Yanchihe phosphorus mine," *Hydrogeology and Engineering Geology*, vol. 1, pp. 1–7, 1983.

[8] Z. Zhang, S. Wang, D. Nie, H. Liu, Y. Li, and J. Xu, *Study on Major Engineering Geological Problems of Longyangxia Hydropower Station*, Chengdu University of Science and Technology Press, Chengdu, 1989.

[9] C. Zhu, M. He, M. Karakus, X. Cui, and Z. Tao, "Investigating toppling failure mechanism of anti-dip layered slope due to excavation by physical modelling," *Rock Mechanics and Rock Engineering*, vol. 53, no. 11, pp. 5029–5050, 2020.

[10] D. P. Adhikary and A. V. Dyskin, "Modelling of progressive and instantaneous failures of foliated rock slopes," *Rock Mechanics and Rock Engineering*, vol. 40, no. 4, pp. 349–362, 2007.

[11] D. N. Petley, M. H. Bulmer, and W. Murphy, "Patterns of movement in rotational and translational landslides," *Geology*, vol. 30, no. 8, pp. 719–722, 2002.

[12] A. L. Handwerger, E. J. Fielding, M.-H. Huang, G. L. Bennett, C. Liang, and W. H. Schulz, "Widespread initiation, reactivation, and acceleration of landslides in the northern California coast ranges due to extreme rainfall," *Journal of Geophysical Research: Earth Surface*, vol. 124, no. 7, pp. 1782–1797, 2019.

[13] M. Dong, F. Zhang, J. Lv, M. Hu, and Z. Li, "Study on deformation and failure law of soft-hard rock interbedding toppling slope base on similar test," *Bulletin of Engineering Geology and the Environment*, vol. 79, no. 9, pp. 4625–4637, 2020.

[14] M. Dong, F. Zhang, M. Hu, and C. Liu, "Study on the influence of anchorage angle on the anchorage effect of soft-hard interbedded toppling deformed rock mass," *KSCE Journal of Civil Engineering*, vol. 24, no. 8, pp. 2382–2392, 2020.

[15] Z. Tao, Q. Geng, C. Zhu et al., "The mechanical mechanisms of large-scale toppling failure for counter-inclined rock slopes," *Journal of Geophysics and Engineering*, vol. 16, no. 3, pp. 541–558, 2019.

[16] D. N. Petley, D. J. Petley, and R. J. Allison, "Temporal prediction in landslides-understanding the Saito effect," in *Presented at The Tenth International Symposium on Landslides and Engineered Slopes, Xi'an, China*, pp. 886–892, CRC Press, London, 2008.

[17] S. Qin, J. Jiao, and Z. Li, "Nonlinear evolutionary mechanisms of instability of plane-shear slope: catastrophe, bifurcation, chaos and physical prediction," *Rock Mechanics and Rock Engineering*, vol. 39, no. 1, pp. 59–76, 2006.

[18] X. Wang, "Geological properties of large-scale highspeed landslides and their mechanism models," *Bulletin of Engineering Geology and the Environment*, vol. 43, no. 1, pp. 93–99, 1991.

[19] C. Liu and R. Xiao, "Mechanism analysis on Yanchihe avalanche disaster in Yuan'an, Hubei," *Journal of Catastrophology*, vol. 36, no. 2, pp. 130–133+150, 2021.

[20] H. Liu and Z. Zhang, "The mechanism of hugh landslides in overconsolidated clay near Longyang gorge damsite," *Journal of Chengdu College of Geology*, vol. 13, no. 3, pp. 94–104, 1986.

[21] T. Li, *Research on the Mechanism of Mountainous Landslide Geohazrds Induced by Underground Mining*, University of Chinese Academy of Sciences, 2014.

[22] F. Meng, H. Zhou, C. Zhang, R. Xu, and J. Lu, "Evaluation methodology of brittleness of rock based on post-peak stress–strain curves," *Rock Mechanics and Rock Engineering*, vol. 48, no. 5, pp. 1787–1805, 2015.

[23] F. Renard, J. McBeck, N. Kandula, B. Cordonnier, P. Meakin, and Y. Ben-Zion, "Volumetric and shear processes in crystalline rock approaching faulting," *Proceedings of the National Academy of Sciences*, vol. 116, no. 33, pp. 16234–16239, 2019.

[24] H. Chen, S. Qin, L. Xue, and C. Xu, "Why the Xintan landslide was not triggered by the heaviest historical rainfall: mechanism and review," *Engineering Geology*, vol. 294, article 106379, 2021.

[25] H. Chen, S. Qin, L. Xue, B. Yang, and K. Zhang, "A physical model predicting instability of rock slopes with locked segments along a potential slip surface," *Engineering Geology*, vol. 242, pp. 34–43, 2018.

[26] C. Zhu, X. Xu, X. Wang et al., "Experimental investigation on nonlinear flow anisotropy behavior in fracture media," *Geofluids*, vol. 2019, Article ID 5874849, 9 pages, 2019.

[27] Z. T. Bieniawski, "Time-dependent behaviour of fractured rock," *Rock Mechanics*, vol. 2, no. 3, pp. 123–137, 1970.

[28] H. Li, Y. Qiao, R. Shen et al., "Effect of water on mechanical behavior and acoustic emission response of sandstone during loading process: phenomenon and mechanism," *Engineering Geology*, vol. 294, article 106386, 2021.

[29] B. Yang, S. Qin, L. Xue, and H. Chen, "The reasonable range limit of the shape parameter in the Weibull distribution for describing the brittle failure behavior of rocks," *Rock Mechanics and Rock Engineering*, vol. 54, no. 6, pp. 3359–3367, 2021.

[30] L. Xue, S. Qin, X. Pan, H. Chen, B. Yang, and K. Zhang, "Mechanism and physical prediction model of instability of the locked-segment type slopes," *Journal of Engineering Geology*, vol. 26, no. 1, pp. 179–192, 2018.

[31] D. M. Cruden, "Major rock slides in the rockies," *Canadian Geotechnical Journal*, vol. 13, no. 1, pp. 8–20, 1976.

[32] R. Huang, G. Chen, F. Guo, G. Zhang, and Y. Zhang, "Experimental study on the brittle failure of the locking section in a large-scale rock slide," *Landslides*, vol. 13, no. 3, pp. 583–588, 2016.

[33] K. Hall and A. Hall, "Weathering by wetting and drying: some experimental results," *Earth Surface Processes and Landforms*, vol. 21, no. 4, pp. 365–376, 1996.

[34] R. A. L. Wray and F. Sauro, "An updated global review of solutional weathering processes and forms in quartz sandstones and quartzites," *Earth-Science Reviews*, vol. 171, pp. 520–557, 2017.

[35] D. K. Keefer, R. C. Wilson, R. K. Mark et al., "Real-time landslide warning during heavy rainfall," *Science*, vol. 238, no. 4829, pp. 921–925, 1987.

[36] M. Urosevic, C. Rodriguez-Navarro, C. V. Putnis, C. Cardell, A. Putnis, and E. Ruiz-Agudo, "In situ nanoscale observations of the dissolution of dolomite cleavage surfaces," *Geochimica et Cosmochimica Acta*, vol. 80, pp. 1–13, 2012.